Spring Harbor Symp. Quant. Biol. **37**, 299 (1972); D. A. D. Parry, *Biosci. Rep.* **2**, 1017 (1982); J. F. Conway and D. A. D. Parry, *Int. J. Biol. Macromol.* **12**, 328 (1990); A. Lupas, M. Van Dyke, J. Stock, *Science* **252**, 1162 (1991); B. Berger, D. B. Wilson, T. Tonchev, M. Milla, P. S. Kim, *Proc. Natl. Acad. Sci. U.S.A.*, in press.

27. pK_a values were determined at 25°C from a nonlinear least-squares fit of the change in chemical shift of the carboxylate ^{13}C-resonance with pH to the Henderson-Hasselbach equation [J. S. Cohen, R. I. Shrager, M. McNeel, A. N. Schechter, *Nature* **228**, 642 (1970)]. The pH was measured at room temperature before and after each NMR experiment and varied by less than 0.05 units. Because the largest source of uncertainty is systematic error in the measurement of pH, the experiments were performed in parallel (folded and unfolded in pairs), which reduces the error in the ΔpK_a values to less than the error in the measurement of the absolute value of any individual pK_a value. pK_a values measured in two independent sets of experiments agreed to within 0.05 units.

28. We are indebted to P. Harbury and B. Tidor for insightful discussions. We thank M. W. Burgess, S. Britt, and R. Rutkowski for peptide synthesis and mass spectrometry. Supported by grant GM44162 from the National Institutes of Health.

12 October, 1994; accepted 21 December, 1994

Nicotinic Receptor Binding Site Probed with Unnatural Amino Acid Incorporation in Intact Cells

Mark W. Nowak, Patrick C. Kearney, Jeffrey R. Sampson, Margaret E. Saks, Cesar G. Labarca, Scott K. Silverman, Wenge Zhong, Jon Thorson, John N. Abelson, Norman Davidson, Peter G. Schultz, Dennis A. Dougherty, Henry A. Lester*

The nonsense codon suppression method for unnatural amino acid incorporation has been applied to intact cells and combined with electrophysiological analysis to probe structure-function relations in the nicotinic acetylcholine receptor. Functional receptors were expressed in *Xenopus* oocytes when tyrosine and phenylalanine derivatives were incorporated at positions 93, 190, and 198 in the binding site of the α subunit. Subtle changes in the structure of an individual side chain produced readily detectable changes in the function of this large channel protein. At each position, distinct features of side chain structure dominated the dose-response relation, probably by governing the agonist-receptor binding.

In the study of membrane-bound receptor, channel, and transporter proteins, classical pharmacology has defined highly specific agonists and antagonists, and quantitative structure-activity studies have generated many hypotheses concerning ligand-receptor interactions. More recently, the combination of site-directed mutagenesis and heterologous expression has enabled functional studies of the consequences of structural modifications of the receptors. In the absence of atomic-scale structural data for membrane-bound receptors, these methods provide detailed information for the study of ligand-receptor interactions. First-generation mutagenesis methodologies used the normal translation machinery in such a way that a residue of interest could be changed to any of the other 19 natural amino acids.

Site-directed mutagenesis combined with nonsense suppressors [transfer RNAs (tRNAs) altered at the anticodon so that they insert an amino acid in response to an mRNA termination codon] have allowed the generation of several proteins with known amino acid changes from a single mRNA (*1*). Recently, second-generation mutagenesis methodologies have incorporated the nonsense suppression principle and extended the amino acid repertoire by providing a means for the site-specific incorporation of unnatural amino acids into proteins in cell-free systems (*2*, *3*). We report here the adaptation of this approach to a heterologous expression system in an intact cell. Combined with the high sensitivity and resolution of modern electrophysiological techniques, the incorporation of unnatural amino acids provides a general method for structure-function studies of receptors, channels, and transporters.

Figure 1A outlines the nonsense codon–tRNA suppressor method as adapted to intact eukaryotic cells. A *Xenopus* oocyte was coinjected with two mutated RNA species: (i) mRNA, synthesized in vitro from a mutated complementary DNA (cDNA) clone containing a stop codon, TAG, at the amino acid position of interest and (ii) a suppressor tRNA (*4*) containing the complementary anticodon sequence (CUA) and the desired unnatural amino acid synthetically acylated to the 3′ end (*5*, *6*). During translation by the oocyte's synthetic machinery, the unnatural amino acid was specifically incorporated at the appropriate position in the protein encoded by the mRNA.

We exploited this method to study a ligand-gated ion channel, the nicotinic acetylcholine (ACh) receptor (*7*). The muscle-type ACh receptor (AChR) contains five subunits with a stoichiometry of $\alpha_2\beta\gamma\delta$. An appropriate subject for this first investigation was the interaction between ligands

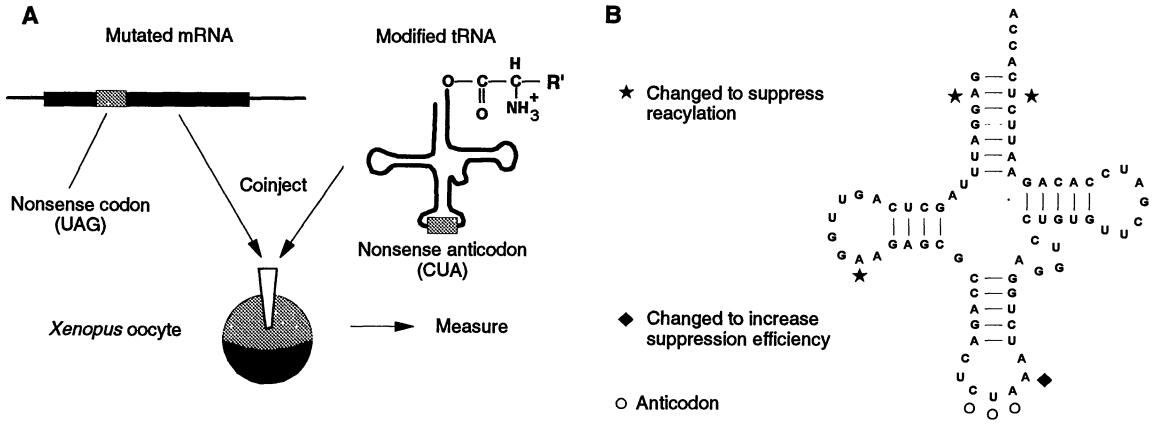

Fig. 1. (**A**) Strategy for unnatural amino acid incorporation into membrane proteins of intact *Xenopus* oocytes. The mRNA was generated from a cDNA clone in which the codon of interest had been mutated to a nonsense codon, TAG. The unnatural side chain is denoted as R′. (**B**) Structure of the nonsense suppressor tRNA-MN3, designed to maximize suppression efficiency and to minimize reacylation.

and the amino acid residues in the α subunit at positions 93, 190, and 198. There is good evidence (though not conclusive proof) that these residues contribute to the agonist-binding pocket (*8*). The wild-type residue is tyrosine at each of these positions in nearly all known AChR α subunits (*9*). Previous studies have shown that phenylalanine at these positions modifies the binding of ACh, with minimal effects on the subsequent conformational change that opens the channel (*10*). The binding of *d*-tubocurarine (dTC) and several other competitive antagonists is also affected by mutations at these positions (*11*). We examined several measures of receptor function as affected by the incorporation of various tyrosine and phenylalanine derivatives (Fig. 2) at positions 93, 190, and 198.

A major concern from the outset was possible reacylation of the injected suppressor tRNA with natural amino acids by endogenous aminoacyl-tRNA synthetases (aaRs). Reacylation could occur after delivery of the nonnatural amino acid to the ribosome or by means of a synthetase editing mechanism (*12*) that removes the unnatural amino acid and replaces it with a natural one. Either type of reacylation would lead to an uncontrollable mixture of amino acids at the site of interest in the protein. Therefore, a tRNA amber suppressor (anticodon CUA; tRNA-MN3) having a low probability of reacylation by each of the 20 synthetases in the cell (Fig. 1B) was designed by alteration of a yeast $tRNA^{Phe}_{CUA}$ used previously to incorporate unnatural amino acids in an in vitro translation system (*2*). Two changes made previously in yeast $tRNA^{Phe}$ (G34C and A35U) introduced the amber anticodon and removed known recognition elements for eukaryotic phenylalanyl-tRNA synthetases (PheRS) (*13*). However, these changes also introduced a recognition site for TyrRS and for GlnRS. Because the wild-type C2-G71 base pair could also contribute to recognition by TyrRS and GlnRS (*14*), this base pair was changed to A-U in tRNA-MN3. In addition, the G20A mutation was introduced to decrease reacylation by PheRS. Like the original yeast $tRNA^{Phe}_{CUA}$, tRNA-MN3 also contains the G37A mutation to increase suppression efficiency (*15*).

We first estimated, using in vitro translation of the AChR α subunit in a reticulocyte lysate system (*16*), that the incorporation efficiency was on the order of 10% for several unnatural amino acids (*17*, *18*). If this efficiency applies to translation in intact *Xenopus* oocytes as well (*19*, *20*), one would expect generation of full-length α subunits to be rate-limiting for the production of oligomeric receptors. Because two α subunits are incorporated into each complex, 10- to 100-fold greater amounts of α subunit mRNA, relative to β, γ, and δ subunit mRNAs, were injected.

To test the efficacy and fidelity of unnatural amino acid mutagenesis in oocytes, we incorporated into the α subunit (i) the natural tyrosine residue at position 190, (ii) the natural tyrosine at position 198, or (iii) a phenylalanine at position 198. Currents of tens to hundreds of nanoamperes were observed at −80 mV as soon as 6 hours after injection, and currents generally greater than 1 μA were observed 24 hours after injection. Electrophysiological properties of the expressed receptors were identical to those of the wild-type receptor (Fig. 3, A and B) or of the previously studied $\alpha Tyr^{198} \rightarrow Phe^{198}$ (αTyr198Phe) (*21*) mutant generated by conventional mutagenesis (Fig. 3D). Thus, the method yields the expected data when compared with conventional mutagenesis and heterologous expression. There were no responses when no tRNA at all was injected.

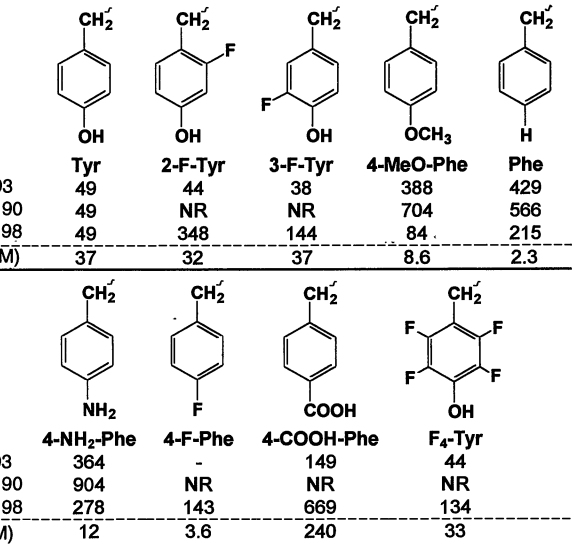

		Tyr	2-F-Tyr	3-F-Tyr	4-MeO-Phe	Phe
EC_{50} for ACh (μM)	93	49	44	38	388	429
	190	49	NR	NR	704	566
	198	49	348	144	84	215
dTC K_i (nM)		37	32	37	8.6	2.3

		4-NH_2-Phe	4-F-Phe	4-COOH-Phe	F_4-Tyr
EC_{50} for ACh (μM)	93	364	-	149	44
	190	904	NR	NR	NR
	198	278	143	669	134
dTC K_i (nM)		12	3.6	240	33

Fig. 2. Natural and unnatural side chains yielding functional receptors at positions 93, 190, and 198; and summary of ACh dose-response relations and dTC inhibition data (position 198 only) for these side chains. Mean values are given for at least six dose-response relations (EC_{50}) or dose-ratio analyses (K_i) from at least two batches of oocytes. The SEM ranged from 8 to 12% of the mean for EC_{50} values less than 600 μM and was 15 to 20% of the mean for higher values. NR, no detectable response; dashes, not tested.

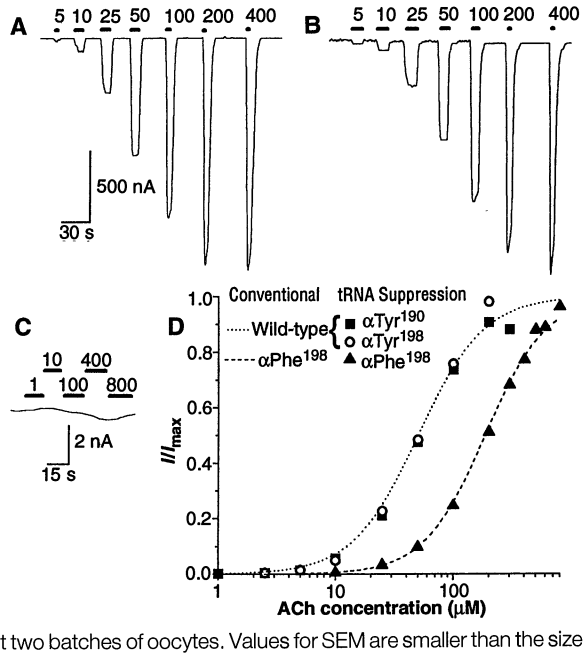

Fig. 3. Validation of the nonsense suppression technique for intact cells. (A) and (B) show reconstruction of the wild-type AChR. ACh-induced currents are shown from oocytes injected with AChR β, γ, and δ subunit mRNAs plus (**A**) wild-type α subunit mRNA, (**B**) α198TAG mRNA plus Tyr–tRNA-MN3, or (**C**) α198TAG mRNA plus full-length unacylated tRNA. ACh applications are shown by horizontal bars; concentrations are micromolar. (**D**) Validation by comparison with conventional site-directed mutagenesis. Tyr (the wild-type residue) or Phe was incorporated at positions α190 and α198. Dotted and dashed lines represent dose-response relations for the wild-type AChR and for AChRα Tyr198Phe obtained by conventional mutagenesis, respectively. Data points represent the tRNA suppression technique. Each point is the mean of four to eight measurements from at least two batches of oocytes. Values for SEM are smaller than the size of the symbols.

M. W. Nowak, J. R. Sampson, M. E. Saks, C. G. Labarca, J. N. Abelson, N. Davidson, H. A. Lester, Division of Biology, California Institute of Technology, Pasadena, CA 91125, USA.
P. C. Kearney, Division of Biology and Division of Chemistry and Chemical Engineering, California Institute of Technology, Pasadena, CA 91125, USA.
S. K. Silverman, W. Zhong, D. A. Dougherty, Division of Chemistry and Chemical Engineering, California Institute of Technology, Pasadena, CA 91125, USA.
J. Thorson and P. G. Schultz, Howard Hughes Medical Institute, Department of Chemistry, University of California, Berkeley, CA 94720, USA.
*To whom correspondence should be addressed.

The most important control experiment involved coinjection of the full-length but unacylated tRNA-MN3 with the mRNA, because oocytes's endogenous synthetases can acylate injected tRNAs (*22*). In 19 out of 20 experiments, each involving 5 to 10 oocytes and typified by Fig. 3C, no response at concentrations as high as 800 μM ACh was seen up to 24 hours after injection. In contrast, after injection of the unacylated $tRNA^{Phe}_{CUA}$, there were detectable responses in the 10- to 50-nA range for about half the oocytes after 24 hours. After 48 hours, responses with unacylated $tRNA^{Phe}_{CUA}$ were two- to fourfold larger than the 10- to 30-nA signals observed with unacylated tRNA-MN3 (*23*). Thus, we conclude that reacylation is not a distorting factor with tRNA-MN3 and that all functioning channels contain only the desired residue at the mutation site in the α subunit.

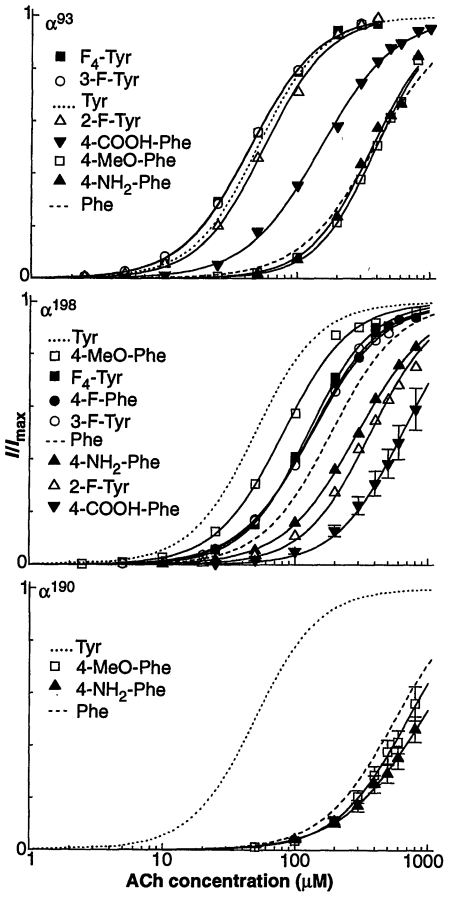

Fig. 4. Normalized dose-response relations for ACh receptors containing unnatural side chains at one of three positions (93, 198, or 190) in the α subunit. The symbols for the unnatural residues are consistent among the three panels, but the order of symbols in the key for each panel follows the rank order of EC_{50} values. The wild-type residue is Tyr in each case, and the wild-type dose-response relation is superimposed as a dotted line. The data for Phe at each position were obtained by both conventional mutagenesis and the nonsense suppression method (see Fig. 3D) and are superimposed as dashed lines. Each symbol represents measurements on at least five oocytes from at least two separate batches. Individual dose-response relations were fit to the Hill equation, I/I_{max} $1/\{1 + (EC_{50}/[A])^{n_H}\}$, where I is the current for agonist concentration $[A]$, I_{max} is the maximum current, EC_{50} is the concentration to elicit a half-maximum response, and n_H is the Hill coefficient. Values for n_H ranged from 1.6 to 1.8. I_{max} values exceeded 500 nA in all cases except for 4-NH_2-Phe at position 190, where I_{max} was ~100 nA. Values for SEM are shown where they exceed the size of the symbols.

We then studied receptors containing a variety of unnatural amino acids at positions 93, 198, and 190 (Figs. 2 and 4). These receptors display many characteristics similar to those of wild-type receptors, including responses to ACh in the micromolar concentration range and Hill coefficients near 2, which suggests that the open state of the channel is much more likely to be associated with the presence of two bound agonist molecules than with a single bound agonist. In addition, receptors containing unnatural amino acid residues are inhibited in a competitive fashion by dTC. Limited kinetic measurements have also been made; voltage-jump relaxations at ACh concentrations equal to the half-maximal effective concentration (EC_{50}) with αTyr^{198}(4-MeO-Phe) displayed rate constants (0.084 to 0.090 ms^{-1}) near that of the wild-type receptor (*24*). These rate constants equal the sum of rate constants for initiating and terminating a burst of single-channel openings (*25*); therefore, the unnatural amino acid residues produced no major changes in the kinetics of channel gating, which is consistent with previous measurements on the conventional αTyr198Phe mutation (*11*). Also, receptors containing unnatural side chains displayed desensitization on the same time scale as did wild-type receptors.

There were, however, variations in the dose-response relation for ACh among the mutants at all the sites. For example, at 50 μM ACh, the normalized responses covered a range of nearly 100-fold and EC_{50} values ranged over nearly 10-fold.

Our results for unnatural amino acid residues at position 93 establish a prominent role for the hydroxyl group of the wild-type tyrosine (Figs. 2 and 4). It is surprising that all side chains with 4′-hydroxyl groups show comparable EC_{50} values, despite the wide range of pK_a values expected for these residues (10, 9.2, 8.7, and ~5 for Tyr, 3-F-Tyr, 2-F-Tyr, and F_4-Tyr, respectively) (*26*). The most straightforward explanation of this result is that all Tyr derivatives are in the same protonation state and that this state is OH, not O^-. There is ample precedent for elevated pK_a values in hydrophobic protein environments (*27*), and apparently this is the case with the agonist binding site. In this light, 4-COOH-Phe (pK_a ~4) can also be considered as contributing an OH group, but perhaps with suboptimal positioning. These results, in combination with the observation that 4-MeO-Phe responds no better than Phe itself, indicate that an aromatic OH at position 93 functions as a hydrogen bond donor.

The rank order of agonist EC_{50} for the modifications at position 198 differs markedly from that at position 93. Therefore, these two tyrosines are involved in qualitatively different interactions with the agonist. The observation that 4-MeO-Phe at position 198 responds to ACh almost as effectively as does Tyr at this position rules out both hydrogen bond donation and deprotonation as important characteristics of this side chain. In addition, neither hydrophobicity scales nor any of the well-known parameters that model aromatic substituent effects (*28*) rationalize the data for the agonist at the α198 residue, which suggests that the substituent on the aromatic ring is not the primary contributor to agonist recognition at this position. As a preliminary model, we ascribe this role to the aromatic ring of Tyr^{198} interacting with the quaternary ammonium group of ACh (*10, 11*) through a cation-π interaction (*29*), as suggested for acetylcholinesterase (*30*). Of course, some of the variations measured at this and the other sites could result from indirect effects of side chain structure, such as displacement of neighboring residues.

In experiments on competitive blockade (*31*) by dTC of receptors containing unnatural amino acids at the α198 position (Fig. 2), apparent dissociation constants for inhibition, K_i, range over a factor of 100. The rank order of dTC K_i values differs considerably from that for agonist EC_{50}, amplifying and extending previous observations made by means of conventional mutagenesis. The present data support suggestions (*10, 11*) that the interaction between the residue at α198 and curare is predominantly hydrophobic.

At position 190, only Phe, 4-MeO-Phe, and 4-NH_2-Phe produce detectable responses; and the EC_{50} for these groups was more than 10-fold greater than that for the wild-type receptor. Position 190 is therefore the most sensitive to structural modifications of the three positions we have studied.

The versatility in substitutions made possible by unnatural amino acid incorporation can now be applied to studies in intact cells, in particular for membrane receptors. Subtle chemical changes in the structure of an individual side chain result in readily detectable changes in the function of a large receptor/channel protein, providing decisive tests for previous hypotheses concerning ligand-receptor interactions. These initial studies have emphasized fairly conservative mutations in order to establish the viability

of the method. However, in cell-free systems, unnatural amino acid incorporation has been used not only to modify side chains, but also to substitute nonpeptide linkages for the peptide bond and to incorporate fluorescent, photolabile, and spin-labeled moieties (*2*). These tactics can now be applied to many questions concerning structural and functional aspects of ion channels, receptors, and transporters.

REFERENCES AND NOTES

1. J. Normanly *et al.*, *Proc. Natl. Acad. Sci. U.S.A.* **83,** 6548 (1986); M. L. Michaels *et al.*, *ibid.* **87,** 3957 (1990).
2. C. J. Noren *et al.*, *Science* **244**, 182 (1989); S. A. Robertson *et al.*, *J. Am. Chem. Soc.* **113**, 2722 (1991); D. Mendel *et al.*, *ibid.*, p. 2758; J. A. Ellman *et al.*, *Methods Enzymol.* **202**, 301 (1992); V. W. Cornish *et al.*, *Proc. Natl. Acad. Sci. U.S.A.* **91**, 2910 (1994).
3. J. D. Bain, C. G. Glabe, T. A. Dix, R. A. Chamberlain, *J. Am. Chem. Soc.* **111**, 8013 (1989).
4. The gene for tRNA-MN3, flanked by an upstream T7 promoter and a downstream Fok I restriction site, was constructed from eight overlapping DNA oligonucleotides and cloned into pUC19. Digestion of the resulting plasmid (pMN3) with Fok I gave a linearized DNA template corresponding to the tRNA transcript, tRNA-MN3, shown in Fig. 1B minus the CA at positions 75 and 76. In vitro transcription of Fok I–linearized pMN3 was done as described [J. R. Sampson and O. C. Uhlenbeck, *Proc. Natl. Acad. Sci. U.S.A.* **85,** 1033 (1988)]. The 74-nucleotide tRNA transcript, tRNA-MN3 (minus CA), was purified to single-nucleotide resolution by denaturing polyacrylamide electrophoresis and then quantitated by ultraviolet absorption [J. R. Sampson and M. E. Saks, *Nucleic Acids Res.* **21,** 4467 (1993)]. Digestion of pMN3 with Bst NI gave the template for transcription of the full-length tRNA.
5. Most unnatural amino acids were purchased from commercial sources. For the preparation of 4-COOH-Phe, an appropriately protected (NVOC = nitroveratryloxycarbonyl) Tyr [NVOC-Tyr(OH)-OtBu] was converted to the triflate [NVOC-Tyr(OTf)-OtBu]. A mixture of the trislate, KOAc, $Pd(OAc)_2$, 1,1′-bis-(diphenylphosphino)ferrocene (dppf), and dimethylsulfoxide (DMSO) was reacted at 85°C by means of a Pd-catalyzed carbonylation sequence that was quenched with HCl [see S. Cacchi and A. Lupi, *Tetrahedron Lett.* **33**, 3939 (1992)]. The synthesis of dCA and the procedure for coupling the amino acid are described in (*2*).
6. The dCA-amino acids were coupled to tRNA-MN3 (minus CA) according to the method of T. E. England, A. G. Bruce, and O. C. Uhlenbeck [*Methods Enzymol.* **65**, 65 (1980)]. Before ligation with T4 RNA ligase, tRNA-MN3 (minus CA) was heated to 90°C in 6 mM Hepes-KOH (pH 7.5) for 3 min and slowly cooled to room temperature. Gel-shift analysis indicated approximately 75% efficiency in ligation, which was independent of the identity of the dCA–amino acid donor.
7. J.-L. Galzi, F. Revah, A. Bessis, J.-P. Changeux, *Annu. Rev. Pharmacol.* **31**, 37 (1991); H. A. Lester, *Annu. Rev. Biophys. Biomol. Struct.* **21,** 267 (1992); A. Karlin, *Curr. Opin. Neurobiol.* **3**, 299 (1993).
8. M. J. Dennis *et al.*, *Biochemistry* **27**, 2346 (1988); S. N. Abramson *et al.*, *J. Biol. Chem.* **264**, 12666 (1989); J.-L. Galzi *et al.*, *ibid.* **265**, 10430 (1990); J. B. Cohen *et al.*, *ibid.* **266**, 23354 (1991).
9. A search of the GenBank database reveals that the sole exception is the neuronal α^5 subunit.
10. G. F. Tomaselli *et al.*, *Biophys. J.* **60**, 721 (1991); M. L. Aylwin and M. M. White, *Mol. Pharmacol.* **46**, 1149(1994).
11. M. E. O'Leary *et al.*, *Am. J. Physiol.* **266**, C648 (1994); S. M. Sine *et al.*, *J. Biol. Chem,* **269,** 8808 (1994).
12. S. X. Lin, M. Batzinger, P. Remy, *Biochemistry* **23**, 4109 (1984).
13. J. Sampson *et al.*, *ibid.* **31,** 4161 (1992); I. A. Nazarenko *et al.*, *Nucleic Acids Res.* **20**, 475 (1992).
14. M. Jahn *et al.*, *Nature* **352**, 258 (1991); M. A. Rould *et al.*, *Science* **246**, 1135 (1989).
15. M. Yarus, *Science* **218**, 646 (1982).
16. A rabbit reticulocyte lysate system (Promega, Madison, WI) was used with incorporation of [^{35}S]methionine.
17. Site-directed mutagenesis was carried out with the Clontech Transformer site-directed mutagenesis kit (Palo Alto, CA). The α, β, γ, and δ subunits of AChR were subcloned into pAMV-PA, a modified pBS (S/K$^+$) vector containing an alfalfa mosaic virus (AMV) region directly upstream from the coding region of the insert and an A_{50} sequence downstream from the insert. The AMV region binds ribosomes tightly and increases expression [S. A. Jobling and L. Gehrke, *Nature* **325**, 622 (1987)], and we find that it is effective in both the in vitro translation and oocyte expression systems. Capped transcripts were prepared in vitro.
18. Before in vitro translation or microinjection, the NVOC–aminoacyl–tRNA-MN3 was renatured by incubation at 65°C for 3 min. The NVOC protecting group was subsequently removed by irradiation of the sample for 5 min at 23°C with a 1-kW Xenon lamp using WG-335 and UG-11 filters (Schott, Duryea, PA). The deprotected aminoacyl–tRNA-MN3 was immediately mixed with the desired mRNA and either added to the in vitro translation reaction or microinjected into *Xenopus* oocytes.
19. In the δ subunit of mouse AChR, TAG is the stop codon. To prevent the aminoacylated tRNA from inserting an amino acid at this position, this sequence was mutated to TGA.
20. Deprotected aminoacylated tRNAs were mixed with the desired AChR αTyr93TAG, αTyr190TAG, or αTyr198TAG mRNA (10:1:1:1 to 100:1:1:1) and microinjected into *Xenopus* oocytes (50 nl per oocyte) [M. W. Quick and H. A. Lester, in *Ion Channels of Excitable Cells*, T. Narahashi, Ed. (Academic Press, San Diego, CA, 1994), pp. 261–279]. Injected tRNA and mRNA concentrations were 0.4 ng/nl and 0.30 ng/nl, respectively. Wild-type AChR, AChR αTyr190Phe, and AChR αTyr198Phe (4:1:1:1) mRNAs were injected at concentrations of 0.035 mg/ml and 0.35 mg/ml. Electrophysiological recordings were carried out 12 to 24 hours after injection with the use of a two-electrode voltage clamp circuit. Electrode resistance was 0.5 to 1.0 megohm. Bath solutions contained 96 mM NaCl, 2 mM KCl, 1 mM $MgCl_2$ and 5 mM Hepes (pH 7.5). To prevent activation of the endogenous Ca^{2+}-activated Cl^- channel by muscarinic receptors, atropine (1 μM) was included in the bath solution and Ca^{2+} was omitted. Wild-type mRNA synthesized from the AMV vector generally gave EC_{50}values approximately two times greater than those obtained with mRNA synthesized from pBluescript. We have not systematically studied this effect.
21. Abbreviations for the amino acid residues are as follows: A, Ala; C, Cys; D, Asp; E, Glu; F, Phe; G, Gly; H, His; I, Ile; K, Lys; L, Leu; M, Met; N, Asn; P, Pro; Q, Gln; R, Arg; S, Ser; T, Thr; V, Val; W, Trp; and Y, Tyr.
22. M. Bienz, E. Kubli, J. Kohli, S. de Henau, H. Grosjean, *Nucleic Acids Res.* **8**, 5169 (1980).
23. After 3 days, responses with tRNA–pMN-3 tRNA were eight times smaller than with $tRNA^{Phe}_{CUA}$.
24. The membrane potential was stepped from the holding value of −80 mV to +50 mV for 100 ms, followed by a step to a test potential between +50 and −120 mV for 100 ms. Measurements were carried out at 12°C.
25. P. R. Adams, *J. Membr. Biol.* **58**, 161 (1981).
26. J. S. Thorson, J. K. Judice, E. Chapman, E. C. Murphy, P. G. Schultz, *J. Am. Chem. Soc.* in press.
27. D. W. Urry *et al.*, *ibid.* **115,** 7509 (1993).
28. J. P. Hammett, *ibid.* **59**, 96 (1937). For reviews, see R. D. Topsom, *Prog. Phys. Org. Chem.* **12**, 1 (1976); S. H. Unger and C. Hansch, *ibid.*, p. 91; L. S. Levitt and H. F. Widing, *ibid.*, p. 119.
29. D. A. Dougherty and D. A. Stauffer, *Science* **250**, 1558 (1990).
30. J. L. Sussman *et al.*, *ibid.* **253**, 872 (1991).
31. K_i values for dTC were determined by dose-ratio analysis in the presence of several dTC concentrations [see K. Yoshii, L. Yu, K. Mixter-Mayne, N. Davidson, H. A. Lester, *J. Gen. Physiol.* **90,** 553 (1987)].

32. We thank V. Cornish, P. Deshpande, O. Uhlenbeck, and Y. Zhang for suggestions; E. Chapman for help with synthesis; and J. Jankowski for help with the measurements. Sponsored by grants from NIH, the Office of Naval Research, the Howard Hughes Medical Institute, the University of California Tobacco-Related Disease Research Project, and the Beckman Institute at Caltech.

8 November 1994; accepted 23 January 1995

TECHNICAL COMMENTS

Patterns of Human Growth

Human growth has generally been assumed to be a continuous process, the cumulative sum of millions of unsynchronized cell replications. In 1978, J. M. Tanner wrote, "Growth is in general a very regular process. Contrary to opinions still sometimes met, growth in height does not proceed by stops and starts . . ." (*1*). Previous studies of human and animal growth support this concept (*2*).

In their report (*3*), M. Lampl *et al.* challenge this view, concluding instead that human linear growth occurs in sudden spurts, separated by long periods with no measurable growth. They measured crown-heel length weekly, semiweekly, or daily in healthy infants and describe brief aperiodic bursts of growth, up to 1.65 cm in a single day, separated by long intervals, up to 63 days, with no measurable growth. Thus, the human infant was proposed to alternate between two states, one with a growth velocity of zero, the other with a mean velocity of 1 cm per day, which would correspond to an annualized velocity of 365 cm per year.

These observations, if correct, would require fundamental revisions in our understanding of growth (*1*, *2*). For example, the model of saltation and stasis proposed by Lampl *et al.* (*3*) implies the existence of previously unsuspected synchronizing mechanisms, presumably hormonal, able to switch cell division on or off simultaneously throughout the organism, but none of the known endocrine regulators of growth fluctuate in such a manner.

We attempted to confirm the hypothesis of saltatory growth with an experimental